# Cavity Enhanced Velocity Modulation Spectroscopy of $C_2H_5^+$

Brian Siller

Prospectus for Prelim Exam

April 15, 2010 1:00 PM

171 Roger Adams Laboratory

University of Illinois at Urbana-Champaign

#### I. INTRODUCTION

Molecular ions are of great interest to astrochemists and theoreticians. Obtaining laboratory spectra of molecular ions is helpful to both of these groups, since it provides crucial information about their structures in a controlled environment. Astronomers can use laboratory spectra to conduct astronomical searches in interstellar gas clouds. Theoreticians can use the structures determined from spectra to test and improve their computational methods; this is especially useful when working with ions that have nonclassical structures, as test molecules, especially ions, tend to be difficult to observe.

The primary problems with observing molecular ions in a laboratory setting are producing them in large enough quantities to observe and distinguishing them from neutral molecules, which are typically several orders of magnitude more abundant. The aim of our research is to develop ever more sensitive and discriminating spectroscopic techniques in order to observe ions that are primarily of astrochemical importance. We are working toward collecting spectra of many different ions, particularly carbocations, to give astronomers spectral line frequencies to enable astronomical searches.

The field of astrochemistry is still quite new. Within the last few decades, astronomers have been working with chemists and physicists to not only discover what molecules are present in the interstellar medium, but also to gain an understanding of how molecular interactions affect the dynamic composition of interstellar clouds. Ions are abundant in interstellar clouds, particularly diffuse clouds, because they are easily ionized by light from stars and cosmic rays; they are also important in many chemical reactions, since rate constants for ion-neutral reactions are generally orders of magnitude greater than those for neutral-neutral reactions.

#### II. PROGRESS

#### A. Cavity Enhanced Absorption Spectroscopy

Our lab has traditionally focused on using continuous-wave cavity ringdown spectroscopy (cw-CRDS) to perform direct absorption spectroscopy of molecules in the gas phase. Although this technique has been successfully used to observe spectra of several molecules, it is somewhat limited by its low duty cycle; by collecting ringdown traces for tens of mi-

croseconds, tens of times per second, the duty cycle is less than 1%. Although it has been demonstrated that the collection rate can be significantly improved [1], this still has a relatively low duty cycle, and is not optimal.

We have improved the duty cycle and the sensitivity of our spectroscopy by abandoning cw-CRDS in favor of cavity-enhanced absorption spectroscopy (CEAS). Rather than sweeping the cavity and only occasionally collecting samples when the cavity and the laser are on resonance, we instead actively lock the cavity length to the laser wavelength. The price we must pay for the improved sensitivity of CEAS is significantly increased experimental complexity.

To keep the cavity on peak resonance with the laser, we use the Pound-Drever-Hall (PDH) technique [2] to generate an error signal that is used in a control loop to lock. The laser is first passed through an electro-optic modulator (EOM) that modulates the phase of the laser light at 14 MHz; this effectively adds sidebands to the laser frequency. The laser is then coupled into an optical cavity, and the back-reflection off of the cavity is reflected by a beamsplitter into a fast detector, as shown in Figure 1. Because this back-reflected beam has interfered with the light within the cavity, it contains information about the resonance of the laser with the cavity, as long as the laser is within  $\pm 14$  MHz of a cavity resonance. The high-frequency components of the signal from this detector are sent into a mixer to be demodulated; the output of the mixer is the error signal, shown in Figures 3 and 4, which is sent to the control electronics that lock the cavity.

Corrections to keep the laser and cavity in resonance with one another are handled by two separate branches of the control loop. The slow loop (which has proportional and integral components) drives the piezo on which one of the cavity mirrors is mounted. The gain of this loop begins to roll off at 70 Hz, where the fast control loop (which is only proportional) begins to take over. The output of the fast loop is sent to a voltage controlled oscillator (VCO), the output of which is amplified and sent to an acousto-optic modulator (AOM) to control the laser wavelength at frequencies up to 65 kHz.

An AOM shifts the frequency of laser light by the RF frequency at which it is driven; for us, this frequency is centered around 85 MHz. It also diverts the beam by an angle  $\theta = \sin^{-1}(\frac{\lambda}{2\Lambda})$ , where  $\lambda$  is the laser wavelength and  $\Lambda$  is the wavelength of sound within the AOM crystal. For our system, where the cavity is positioned approximately 2 m from the AOM, the spatial shift works out to be 0.3 mm·MHz<sup>-1</sup>, which is enough to degrade our

mode-matching to the cavity. To negate this effect, we use a double-pass AOM setup. [3] In this arrangement, shown in Figure 1, the beam is diverted twice, in opposite directions, so any spatial shift is canceled out. Experimentally, we have seen no measurable shift in the beam position when the AOM is tuned over a 30 MHz range.

With the cavity piezo handling the slow corrections to the system, the AOM only needs to make small fast corrections, which have been observed to be around 500 kHz in magnitude. These fast corrections do broaden the effective linewidth of the laser, but the overall laser linewidth is still less than 1 MHz, which is much narrower than our target transition linewidths.

## B. Cavity Enhanced Velocity Modulation Spectroscopy of $\mathrm{N}_2^+$ in a Positive Column

Positive column discharge cells have long been used to spectroscopically study ions. [4] When a high voltage ( $\sim$ 2 kV) is applied across the electrodes, the gas in the cell discharges and forms ions. To distinguish between ions and neutrals, an AC voltage is used; this causes the ions to move back and forth in the cell while the neutrals are unaffected.

Traditionally, a unidirectional multi-pass White Cell has been used to increase the effective path length by a factor of up to  $\sim 10$ . [5] While this has been used to successfully observe spectra of several ions, it is limited in the sensitivity it is capable of obtaining. The path length can't be significantly increased, because longer cells or greater numbers of passes would not be practical, and various noise suppression techniques, such as double-balanced detection, have pushed the noise level as low as possible; so there has been very little recent technological progress on this technique.

To improve our sensitivity, we have developed the technique of cavity-enhanced velocity modulation spectroscopy (CEVMS), in which an optical cavity is placed around a plasma cell, as shown in Figure 2. The cavity length is actively stabilized to stay on resonance with the laser with a PDH locking scheme. Our cavity has a finesse of  $\sim 300$ , limited by the reflectivity of the cavity mirrors and the transmissivity of the Brewster windows on the plasma cell. This allows for a vastly increased effective path length over which the laser interacts with the plasma. Unlike traditional velocity modulation experiments that demodulate the detector signal at the plasma frequency, we demodulate at twice the plasma frequency (2f), due to the symmetric nature of the cavity.

Because we demodulate the detected signal at 2f, the lineshape of the ionic absorptions is observed to be a second derivative of a Gaussian. Any excited neutrals are concentration modulated by the pulsed plasma, but their velocities are not affected by the voltage across the cell, so their lineshapes are Gaussian. The ions and neutrals can also be differentiated by the difference in their phases with respect to the plasma. In our observations,  $N_2^+$  and  $N_2^*$  (an electronically excited state of  $N_2$ ) have appeared 78° out of phase with one another. By using two lock-in amplifiers with different sensitivity and phase settings, we can observe and separate the  $N_2^+$  and  $N_2^*$  signals simultaneously, as shown in Figure 5.

Due to the large laser intensity within the cavity, the perfectly overlapping forward and reverse beams, and the presence of a zero-velocity population of ions, we are able to perform saturation spectroscopy of the ions. By observing Lamb dips, we are able to perform Doppler-free spectroscopy, which allows for much more precise line center determination, and is especially useful when coupled with the precision allowed by an optical frequency comb.

#### C. Optical Frequency Comb

Optical frequency combs provide extremely stable references by heterodyning the optical frequency of the laser down to radio frequencies that can be referenced to very-precise standards. In our system, the comb mode spacing is synchronized to an atomic clock through GPS satellites. Using the comb, we are able to measure the absolute center frequency of our Ti:Sapph laser to within  $\sim 500$  kHz, limited by the jitter and drift in the reference cell to which the laser is locked.

To measure line centers very precisely, we have incorporated an optical frequency comb into our CEVMS instrument. This provides an extremely precise frequency reference for absolute calibration of the spectra we obtain. By using the comb while scanning over Lamb dips, we have determined transition frequencies of  $N_2^+$  to within  $\sim 1$  MHz, which is approximately two orders of magnitude better precision and accuracy than has previously been attained. [6]

#### D. SCRIBES

Over the past several years, our group has been building an ion beam spectrometer that we call SCRIBES (Sensitive Cooled Resolved Ion BEam Spectroscopy). In its present form, ions are produced within an uncooled cathode source, then are collimated and accelerated before going through an asymmetric cylindrical deflector that turns them to be collinear with the laser. By accelerating the ions through several kV before overlapping the ion beam with the laser, the Doppler linewidth is reduced by a factor of  $\sqrt{k_B T/e\Delta V}$  [7]. In practice, the observed linewidth will also be limited by the stability of the voltage source that drives the ion optics; we expect this linewidth to be around 20 MHz.

After  $\sim 30$  cm of collinearity, the ions are turned by a second cylindrical deflector into a custom-built time-of-flight mass spectrometer. The mass spec is used to give us three very important pieces of information about the ion beam: its composition, velocity, and energy spread. Being able to monitor the beam composition real-time allows us to tune the instrument to optimize for a particular molecular ion before attempting to look for it spectroscopically. Knowing the beam velocity allows us to predict the Doppler shift, so we will know at what wavelength to look for spectral lines, and knowing the beam energy spread allows us to anticipate the width of transitions to expect, so we can estimate the sensitivity needed to observe a particular species.

#### III. FUTURE WORK

#### A. Integrating CEVMS with SCRIBES

Now that we have confirmed that CEVMS is an effective spectroscopic technique, the next step is to incorporate it into the ion beam instrument. This should be a fairly straightforward process, as each half of the system has already been shown to work independently. CEVMS has been used to successfully observe several spectral lines of  $N_2^+$  in the positive column discharge cell, and the ion beam has been shown to produce approximately 2  $\mu$ A of beam current through a pair of 4 mm apertures in the drift region, nearly all of which is  $N_2^+$  as measured with the mass spec.

We have placed a metal tube around the drift region of the ion beam, as shown in Figure 6. When a voltage is applied to the tube, the ions slow down, and their absorptions shift according to the equation  $\Delta \nu = \sqrt{\frac{2e\Delta V}{mc^2}}\nu_0$ , where  $\Delta V$  is the voltage drop from the source voltage to the drift tube voltage. [7] By applying a square wave to the tube, the ion beam velocity will be modulated, so the absorption peaks will shift back and forth in wavelength. In our system, a few volts on the drift tube will be enough to shift the absorptions by several MHz, which is more than the expected linewidth. By using a lock-in amplifier to demodulate the signal at the drift tube modulation frequency, we will be able to extract the absorption signal.

#### B. Moving to Mid-IR Spectroscopy

Once we obtain a spectrum of  $N_2^+$ , we will conduct mid-IR spectroscopy with a difference frequency generation (DFG) laser, which has previously been constructed in our lab. By combining Ti:Sapph and Nd:YAG beams in a periodically poled lithium niobate (PPLN) crystal, we obtain a laser that is tunable from 3 to 5 microns, with around 300  $\mu$ W of power.

To retain the very high precision afforded by referencing the Ti:Sapph to the optical frequency comb, we must also stabilize the wavelength of the Nd:YAG. We have achieved this by doubling the frequency of a portion of the YAG with a second-harmonic generation (SHG) crystal, and locking this 532 nm beam to an iodine hyperfine transition using a third-harmonic technique. [8]

Working with the DFG in place of the Ti:Sapph laser provides some additional challenges. Instead of using ordinary photodiode detectors, we will need to use liquid-nitrogen-cooled InSb detectors for both the transmission and back-reflection detectors. The back-reflection detector needs to be fast enough to observe the high-speed modulation required for PDH locking. By reverse-biasing the InSb, we should be able to increase its speed to around 100 MHz. [9]

Our first target to observe with the DFG in the ion beam will be  $H_3^+$ , which has previously been observed in our lab, both in a hollow cathode discharge, and in a supersonic discharge. Once we have the technical aspects of the experiment established, observing  $H_3^+$  should be straightforward.

#### C. Integrating a Supersonic Discharge Source

After observing  $H_3^+$  spectral lines, the next technological step will be integrating the supersonic discharge source, which has been built and tested elsewhere in our lab. [10] The supersonic expansion will be skimmed and transmitted into a differentially-pumped chamber; the rest of the ion optics and ion beam path will remain largely unchanged, with the exception of adding a third cylindrical deflector to the beam path. The adiabatic expansion should allow the ions to cool to a rotational temperature of  $\sim 20$  K before entering the drift region. This has two benefits: greatly simplifying the spectra of any molecules we observe and increasing the intensities of any lines we observe, both due to the reduced rotational partition function.

#### D. Improving Instrument Sensitivity

As we continue to observe new and interesting molecules, we will continue to improve the sensitivity of our spectroscopic techniques. Currently, our locking system has a bandwidth of 65 kHz. It should be possible to improve that up to a few MHz, limited by the response of the AOM. Improving the lock will decrease the noise in our detected signal, and may allow us to move to a higher-finesse cavity. This is extremely advantageous, since any gain in the finesse will translate directly into a gain in the attainable S/N.

To improve the locking bandwidth beyond what the AOM can handle, we can add another EOM to the system. Because an EOM is based on electrical signals, rather than acoustic waves, it can respond to changes orders of magnitude more quickly than an AOM can. When an RF signal is applied to an EOM, it induces a phase shift in the transmitted laser light. By continuously shifting the EOM frequency, it is possible to shift the frequency of the laser. While this can happen quickly (on the order of nanoseconds), it cannot maintain the frequency shift for long, since it will quickly run out of travel, so the AOM must take over and allow the EOM to return to its center position.

The more we increase the bandwidth of the locking system, the more we can increase the cavity finesse, but this will pose some of its own challenges. Currently, the Brewster windows limit the finesse to a maximum of 300; if we want to remove them from the system, we will need to mount the cavity mirrors directly on the vacuum chamber. This can be problematic

for two reasons. First, the turbo pumps that are mounted to the chamber induce vibrations. If the vibrations happen at frequencies that are too high for the cavity piezo to compensate for, the AOM must correct for them; this will cause the linewidth of the laser to broaden. Second, as ions travel along the drift region, some small fraction of them recombine after the first bender but before the second bender. These ions will collide with the cavity mirror and will degrade their reflectivity over time, so we must add a collision cell in front of the cavity mirror. This will increase the ambient pressure in the chamber, thus decreasing the mean free path of the ions of interest and spoiling the efficiency of the ion beam.

If we can overcome these limitations, we will be able to push the finesse of the cavity up by nearly two orders of magnitude, limited by the quality of supermirrors that we can obtain. If we can get to this point, then we will have pushed the signal as high as possible, and any further improvements in sensitivity will need to come from suppressing noise. One possibility is to pursue the noise-immune cavity-enhanced optical heterodyne molecular spectroscopy (NICE-OHMS) technique pioneered by Jun Ye. [11]

In order to implement NICE-OHMS, we will need to add an additional set of sidebands onto the laser, with spacing equal to the free spectral range (FSR) of the cavity; for us, this is  $\sim$ 120 MHz. The most challenging part of this technique is the need to actively keep the sidebands precisely spaced, since the FSR changes as the laser wavelength is scanned.

By coupling the sidebands into the cavity and detecting the beat note between the main band and the sidebands, the detection frequency is essentially increased to 120 MHz, where 1/f experimental noise is extremely small. Any noise in the laser intensity or in the lock between cavity and the laser is identical in all three laser frequencies, it will not affect the final demodulated signal. NICE-OHMS is still prone to low-frequency noise that occurs on time scales on the order of the length of a scan, but we can compensate for that by coupling in our velocity-modulation. By implementing NICE-OHMS, we should be able to approach the shot noise limit.

### E. Spectroscopy of $C_2H_5^+$

#### 1. Motivation & Previous Studies

 $C_2H_5^+$  is the smallest carbocation that can be formed by protonation of a double bond. Unlike related carbocations  $CH_5^+$  [12],  $C_2H_7^+$  [13], and  $C_2H_3^+$  [14], no gas phase spectrum of isolated  $C_2H_5^+$  has been observed. It is a good test molecule for the SCRIBES instrument, since it will allow for the use the DFG with the supersonic expansion ( $C_2H_5^+$  cools much more effectively than  $H_3^+$ ), and it will require the high sensitivity afforded by CEVMS.

The recent Cassini mission to Titan, Saturn's largest moon, included a mass spectrometric analysis of the moon's ionosphere. This analysis showed that  $C_2H_5^+$  is one of the most abundant ions at all sampled altitudes. [15] Recent laboratory experiments simulating Titan's ionosphere with various mixtures of  $N_2$ ,  $CH_4$ ,  $C_2H_2$ , and  $C_2H_4$  have found  $C_2H_5^+$  to be one of the most abundant ions present in all tested gas mixtures. [16]

Its unprotonated form,  $C_2H_4$ , has been detected in IRC+10216, a carbon star that is a rich source of carbon compounds. [17] In the interstellar medium,  $C_2H_5^+$  is expected to be formed primarily by the protonation of ethylene, or by the reaction of methane with either  $CH_3^+$  or  $CH_2^+$ . After it is formed,  $C_2H_5^+$  can form a variety of longer-chain carbocations, such as  $C_3H_3^+$ ,  $C_3H_5^+$ , and  $C_4H_5^+$ . Additionally, it can donate a proton to a multitude of neutral species, or it can dissociatively recombine into smaller neutral molecules, including  $C_2H_4$ ,  $C_2H_2$ ,  $CH_3$  and  $CH_2$ . [18]

Theoretical investigations have shown that then nonclassical bridged-proton strucure of  $C_2H_5^+$  is the only stable conformer in the gas phase. [19, 20] The classical  $H_3C - CH_2^+$  strucure has been calculated to be 30 kJ/mol higher in energy than the nonclassical strucure, and is believed to not even be a local minimum. [21]

Two recent IR photodissociation experiments studying  $C_2H_5^+Ar$  [21] and  $C_2H_5^+Ar_2$  [22] have reported the first experimental confirmation of the bridged-proton structure of  $C_2H_5^+$ . Although the clustering with argon is not expected to significantly affect the molecular geometry, these studies are not useful for guiding astronomical detections, since argon can shift the band center by a few wavenumbers, and no rotational structure was observed in the spectra.

#### 2. Proposed Experiment

While previous experiments could not provide the precision necessary for an astronomical search, they do provide a good starting point for our experiments. We will be able to start with similar discharge conditions  $(C_2H_4/H_2/Ar)$  or  $CH_4/Ar$ , adjust the backing pressure and gas ratios while observing the ion beam with our mass spectrometer, and optimize for production of  $C_2H_5^+$ . These experiments also provide a starting point for our spectral search, since the vibrational bands of Argon-tagged species in the photodissociation experiments are unlikely to be shifted by more than a few wavenumbers.

 $C_2H_5^+$  is an asymmetric top with  $C_{2v}$  symmetry. I propose observing  $\nu_{15}$ , the asymmetric stretching band of the CH<sub>2</sub> moiety. This is a B-type transition, so the rovibrational selection rules are  $\Delta J = 0, \pm 1$ ;  $\Delta K_a = \pm 1$ ;  $\Delta K_c = \pm 1$ . Using these selection rules with rotational constants determined from the geometry given in [20] and the band center observed in [22], the  $\nu_{15}$  band was simulated in PGopher [23] and is shown in Figure 7.

By acquiring a high resolution precision spectrum of  $C_2H_5^+$ , we will provide astronomers with all the information they'll need for conducting astronomical searches for the molecule. With the narrow linewidths observed in the SCRIBES, combined with the sub-MHz precision afforded by the optical frequency comb, we should even be able to predict pure rotational transition frequencies precisely enough to guide microwave studies.

#### IV. CONCLUSIONS

I have developed the technique of cavity-enhanced velocity modulation spectroscopy, and used it to successfully perform ultra-precise sub-Doppler spectroscopy of  $N_2^+$  in a positive column discharge cell. This technique has improved upon the attainable sensitivity compared to cavity ringdown spectroscopy. The next step is to observe  $N_2^+$  in the ion beam, after which we will further improve the instrument by integrating the DFG laser and the supersonic discharge source. We will then acquire rotationally cold, high resolution spectra of many interesting ions, including  $C_2H_5^+$ .

- [1] R. Z. Martínez, M. Metsälä, O. Vaittinen, T. Lantta, L. Halonen, "Laser-locked, high-repetition-rate cavity ringdown spectrometer" *Journal of the Optical Society of America B: Optical Physics* (2006), **23**(4), 727–740.
- [2] R. W. P. Drever, J. L. Hall, F. V. Kowalski, J. Hough, G. M. Ford, A. J. Munley, H. Ward, "Laser phase and frequency stabilization using an optical resonator" *Applied Physics B: Lasers and Optics* (1983), 31(2), 97–105.
- [3] E. A. Donley, T. P. Heavner, F. Levi, M. O. Tataw, S. R. Jefferts, "Double-pass acousto-optic modulator system" *Review of Scientific Instruments* (2005), **76**(6), 063112.
- [4] S. K. Stephenson, R. J. Saykally, "Velocity modulation spectroscopy of ions" *Chemical Reviews* (2005), **105**(9), 3220–3234.
- [5] B. J. McCall, "Spectroscopy of  $H_3^+$  in laboratory and astrophysical plasmas" Ph.D. thesis, University of Chicago (2001).
- [6] D. W. Ferguson, K. N. Rao, P. A. Martin, G. Guelachvili, "High resolution infrared Fourier transform emission spectra of the  $^{14}N_2^+$  Meinel system:  $A^2\Pi_u X^2\Sigma_g^+$ " Journal of Molecular Spectroscopy (1992), **153**, 599–609.
- [7] W. Demtroder, Laser Spectroscopy: Basic Concepts and Instrumentation, 3rd edn., Springer (2003).
- [8] A. J. Wallard, D. C. Wilson, "A digital frequency tripling technique for use in the control system of a frequency stabilized gas laser" Journal of Physics E: Scientific Instruments (1974), 7(3), 161.
- [9] C. M. Lindsay, "Highly sensitive and efficient infrared spectroscopy of molecular ions" Ph.D. thesis, University of Chicago (2002).
- [10] K. Crabtree, "Prospectus: Design of a continuous supersonic expansion discharge source for the acquisition of a rotationally-cold vibrational spectrum of CH<sub>5</sub><sup>+</sup> with the SCRIBES instrument" (2009).
- [11] J. Ye, L.-S. Ma, J. L. Hall, "Ultrasensitive detections in atomic and molecular physics: demonstration in molecular overtone spectroscopy" *Journal of the Optical Society of America B: Optical Physics* (1998), **15**(1), 6–15.
- [12] E. T. White, J. Tang, T. Oka, "CH<sub>5</sub><sup>+</sup>: The infrared spectrum observed" Science (1999),

- **284**(5411), 135–137.
- [13] L. I. Yeh, J. M. Price, Y. T. Lee, "Infrared spectroscopy of the pentacoordinated carbonium ion C<sub>2</sub>H<sub>7</sub><sup>+</sup>" Journal of the American Chemical Society (1989), **111**(15), 5597–5604.
- [14] C. M. Gabrys, D. Uy, M.-F. Jagod, T. Oka, T. Amano, "Infrared spectroscopy of carboions. 8. hollow cathode spectroscopy of protonated acetylene, C<sub>2</sub>H<sub>3</sub><sup>+</sup>," The Journal of Physical Chemistry (1995), 99(42), 15611–15623.
- [15] T. E. Cravens, I. P. Robertson, J. Waite, J. H., R. V. Yelle, W. T. Kasprzak, C. N. Keller, S. A. Ledvina, H. B. Niemann, J. G. Luhmann, R. L. McNutt, W.-H. Ip, V. De La Haye, I. Mueller-Wodarg, J.-E. Wahlund, V. G. Anicich, V. Vuitton, "Composition of Titan's ionosphere" Geophysical Research Letters (2006), 33(7), L07105—.
- [16] R. Thissen, V. Vuitton, P. Lavvas, J. Lemaire, C. Dehon, O. Dutuit, M. A. Smith, S. Turchini, D. Catone, R. V. Yelle, P. Pernot, A. Somogyi, M. Coreno, "Laboratory studies of molecular growth in the Titan ionosphere" *The Journal of Physical Chemistry A* (2009), 113(42), 11211–11220.
- [17] A. Betz, "Ethylene in IRC+10216" Astrophysical Journal (1981), 244, L103-L105.
- [18] J. Woodall, M. Agúndez, A. J. Markwick-Kemper, T. J. Millar, "The UMIST database for astrochemistry 2006" Astronomy and Astrophysics (2007), 466, 1197–1204.
- [19] B. Zurawski, R. Ahlrichs, W. Kutzelnigg, "Have the ions  $C_2H_3^+$  and  $C_2H_5^+$  classical or non-classical structure?" *Chemical Physics Letters* (1973), **21**(2), 309 313.
- [20] W. Quapp, D. Heidrich, "Exploring the potential energy surface of the ethyl cation by new procedures" Journal of Molecular Structure: THEOCHEM (2002), 585(1-3), 105 117.
- [21] H. S. Andrei, N. Solcá, O. Dopfer, "IR spectrum of the ethyl cation: Evidence for the non-classical structure" *Angewandte Chemie International Edition* (2008), **47**(2), 395–397.
- [22] A. M. Ricks, G. E. Douberly, P. v.R. Schleyer, M. A. Duncan, "Infrared spectroscopy of protonated ethylene: The nature of proton binding in the non-classical structure" *Chemical Physics Letters* (2009), **480**(1-3), 17 20.
- [23] C. M. Western, *PGOPHER: A Program for Simulating Rotational Structure*, University of Bristol (2007).

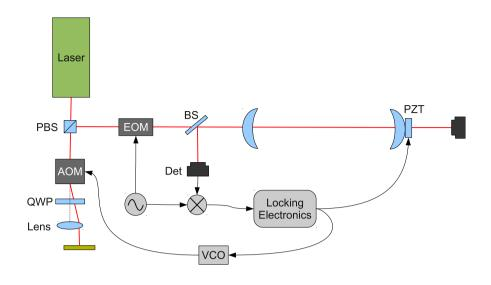


FIG. 1: PDH locking setup

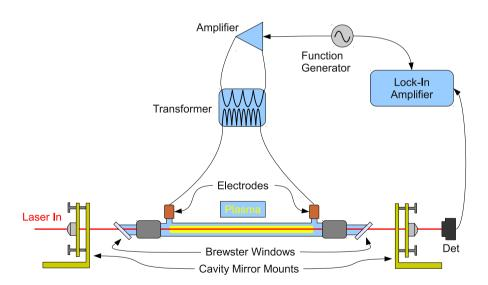


FIG. 2: CEVMS positive column setup

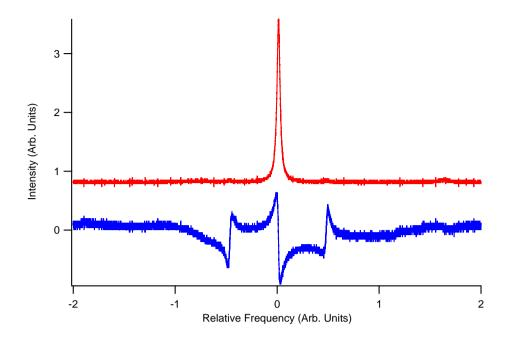


FIG. 3: Cavity transmission (top) and Pound-Drever-Hall error signal (bottom) observed while cavity length is swept

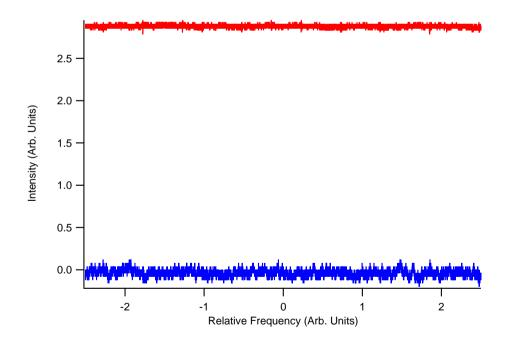


FIG. 4: Cavity transmission (top) and Pound-Drever-Hall error signal (bottom) observed while cavity length is actively locked to the laser wavelength

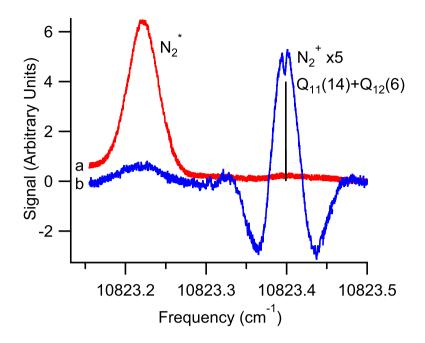


FIG. 5: Representative CEVMS Scan of a)  $\mathrm{N}_2^+$  and b)  $\mathrm{N}_2^*$  in the positive column discharge cell

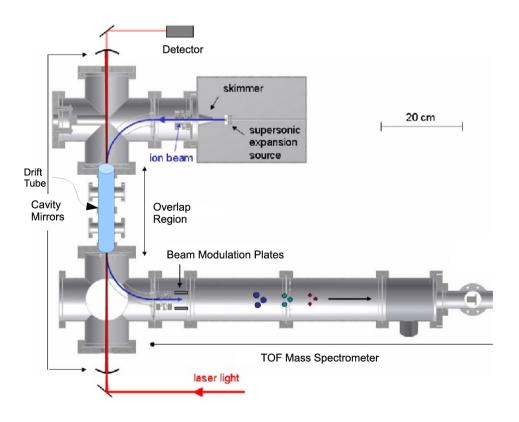


FIG. 6: Scribes Instrument

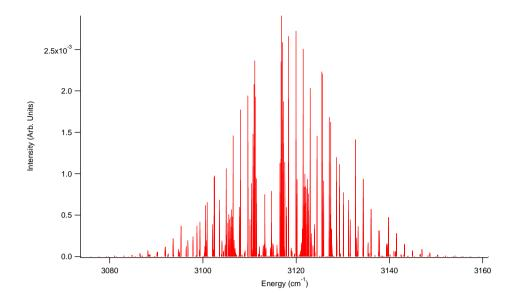


FIG. 7:  $C_2H_5^+$  Spectrum Simulated with PGopher [23] using rotational constants  $A=3.5667~{\rm cm}^{-1}$ ,  $B=0.89946~{\rm cm}^{-1}$ , and  $C=0.79865~{\rm cm}^{-1}$  at a temperature of 20 K